Lake Modeling on Mars for Atmospheric Reconstructions and Simulations (LakeM^{2}ARS): An intermediate-complexity model for simulating Martian lacustrine environments

Eleanor L. Moreland[1], Sylvia G. Dee[1], Yueyang Jiang[1], Grace Bischof[2,3], Michael A. Mischna[2], Nyla Hartigan[1], James M. Russell[4], John E. Moores[3], Kirsten L. Siebach[1]

[1]Rice University Department of Earth, Environmental, and Planetary Sciences, [2]Jet Propulsion Laboratory, California Institute of Technology, [3]York University, [4]Brown University

Key Points

- We present a new intermediate-complexity lake model for simulating paleolake sites on Mars, connecting climate to the geologic record
- Sensitivity experiments with geologic constraints from Gale crater show successful liquid lake conditions in Martian climates
- The open-source model can inform boundary conditions for paleoclimate modeling and improve understanding of the hydrology of early Mars

Abstract

Geomorphic and stratigraphic studies of Mars prove extensive liquid water flowed and pooled on the surface early in Mars' history. Martian paleoclimate models, however, have difficulty simulating climate conditions warm enough to maintain liquid water on early Mars. Reconciling the geologic record and paleoclimatic simulations of Mars is critical to understanding Mars' early history, atmospheric conditions, and paleoclimate. This study uses an adapted lake energy balance model to investigate the connections between Martian geology and climate. The Lake Modeling on Mars for Atmospheric Reconstructions and Simulations (LakeM^{2}ARS) model is modified from an earth-based lake model to function in Martian conditions. We use LakeM^{2}ARS to investigate conditions necessary to simulate a lake in Gale crater. Working at a localized scale, we combine climate input from the Mars Weather Research & Forecasting general circulation model with geologic constraints from *Curiosity* rover observations; in doing so, we identify potential climatic conditions required to maintain a seasonal liquid lake. We successfully model lakes in Gale crater while varying initial climate conditions, lake size, and water salinity. Our results show that ice-free conditions in a plausible Gale crater lake are best supported when the lake is small, ~10 m deep, and air temperatures reach or are just above freezing seasonally during a Martian year. Continued use and iteration of LakeM^{2}ARS will strengthen connections between Mars' paleoclimate and geology to inform climate models and enhance our understanding of conditions on early Mars.

Plain Language Summary

While Mars today is cold and dry, there are many clues on its surface that Mars once had extensive liquid water. When researchers create models to try and understand the climate of

water-rich early Mars, air temperatures are too cold. This suggests water on the surface would have been frozen, which disagrees with available geological evidence. Resolving the disagreement between climate models and Mars' geology would help researchers learn about early Mars' atmosphere, paleoclimate, and hydrologic evolution. We developed the Lake Modeling on Mars for Atmospheric Reconstructions and Simulations (LakeM^{2}ARS) model to simulate lakes on early Mars. Using data collected by the *Curiosity* rover in Gale crater, in-situ observations can inform possible conditions in the Gale lake and connect the geologic record to hydrologic conditions. Our results show that the air temperature needs to reach at least freezing (0°C) during warmer seasons on Mars to melt ice on the lake and create a liquid lake, and this is more achievable when the lake system is smaller. Additional tests using LakeM^{2}ARS will provide stronger connections between climate and geology on early Mars. Such information helps understand what conditions are needed for liquid water and life, or habitability, on other planets.

1. Introduction

Modern Mars is a cold desert world with an atmosphere so thin that water cannot exist stably in liquid form. Orbital imagery of the surface, however, shows geomorphic evidence of long-abandoned river channels, deltas, fans, and dried lake beds (Davis et al., 2019; Fassett & Head, 2008; Wordsworth, 2016). These features indicate a climate that once supported an active hydrological cycle (Carr, 1987; Davis et al., 2019; Fassett & Head, 2008; Wordsworth, 2016). This significant physical evidence, along with chemical observations from orbital and in-situ instruments, suggests that water flowed across and ponded on the surface of Mars repeatedly between its formation 4.5 billion years ago up until at least 3 billion years ago (Goudge et al., 2021; Grotzinger et al., 2015; Palucis et al., 2016; Stucky de Quay et al., 2019).

Since water is a crucial ingredient for life, missions to Mars have targeted landing sites with evidence of past water to explore potentially habitable environments (Golombek et al., 2012; Grant et al., 2018). For example, the Mars Science Laboratory *Curiosity* mission to Gale crater and the Mars 2020 *Perseverance* mission to Jezero crater have found in-situ physical, chemical, and mineralogical evidence that confirms the past presence of surface water flow and lakes in Gale and Jezero craters (Grotzinger et al., 2015; Mangold et al., 2021). Nevertheless, substantial uncertainty remains about how an active hydrological cycle could have been maintained on early Mars. In particular, given Mars' small size, distance from the sun, and uncertain atmospheric composition and density early in its history, it remains a challenge to simulate an active hydrological cycle with general circulation models (GCMs), even when considering a wide range of atmospheric conditions (Kite, 2019; Ramirez & Craddock, 2018; Wordsworth, 2016).

The main challenges in simulating flowing water on early Mars center around the conditions required to warm the planet above the freezing point of water. Mars, ~4 Ga, would have needed a greenhouse effect twice the strength of the present greenhouse effect on Earth to surpass the freezing point and sustain liquid water on the surface (Kite, 2019; Wordsworth, 2016). A leading hypothesis for how early Mars could have experienced amplified warming is with a denser atmosphere and enhanced greenhouse effect; however, the atmosphere of Mars today is extremely thin due to continuous sputtering, photochemical weathering, water sequestration in the crust, and related processes (Jakosky et al., 2018; Scheller et al., 2021). Even when CO_2 is effectively maximized to 2 bar, CO_2 alone does not provide sufficient warming to raise Mars' surface temperature above the freezing point of water (Forget et al., 2013; Kasting, 1991; Kite, 2019).

Estimations for key climatic variables such as air temperature, surface pressure, and obliquity are not well constrained and have wide ranges for early Mars (Kite, 2019; Wordsworth, 2016). Geologic evidence suggests that air temperature on early Mars could have ranged between -18°C to 39°C and surface pressure could have occupied a large range between 0.012 and 2 bar; average present-day surface pressures are around 0.006-0.008 bar, although surface pressures vary quite widely across the planet (Harri et al., 2014; Kite, 2019). Taken together, Mars climate models and present-day geology suggest that early Mars was arid to semi-arid with (at least) intermittent periods of warmer and wetter conditions that could have facilitated an active hydrologic cycle (Kite, 2019; Ramirez & Craddock, 2018).

Several recent commentaries have argued that further progress in understanding water on early Mars requires a new generation of data-model comparisons that directly link geologic constraints to climate model simulations (e.g. Kite, 2019; Wordsworth, 2016). This study progresses toward this goal of using data-model comparison to improve our understanding of Mars' paleoclimate with a case study in Gale crater, Mars. The *Curiosity* rover landed in Gale crater in 2012 to search for conditions necessary to support habitable conditions in Mars' past (Grotzinger et al., 2012). In-situ data from the stratigraphy preserved in Gale crater provide useful constraints for lake model inputs and validation for model outputs. We focus here on the Pahrump Hills section in the Murray Formation within Gale crater, as this stratigraphic section is interpreted to be primarily subaqueous, with lacustrine sedimentation, and data from this area have been used to reconstruct lake stand depth and salinity (Grotzinger et al., 2015; Stack et al., 2019). The Pahrump Hills area is dominated by finely laminated mudstone with some thickly laminated layers, interpreted to result from hyperpycnal flows in a lacustrine setting (Stack et al., 2019). Delta clinoform heights of 1-4 meters in interfingered fluviodeltaic deposits indicate the lake was at least this deep and potentially up to tens of meters deep (Grotzinger et al., 2015). Stratigraphic thickness measurements of ~13 m for the Pahrump Hills section indicate the lake could have existed for as little as 10^3 years, up to 10^7 years (Stack et al., 2019). Furthermore, Stack et al. (2019) employed paleohydraulic modeling for the hyperpycnal river plumes suggested by the Pahrump Hills sedimentology and determined the water salinity needed to be near freshwater to form the observed stratigraphy. Notably, there was a distinct lack of sedimentary evidence for glaciation or extreme cold; however, the possibility exists that the Gale lake was perennially ice covered (Grotzinger et al., 2015; Kling et al., 2020).

Here, we consider the detailed geologic observations of a lake in Gale crater as an opportunity to investigate, on a localized scale, what climatic conditions are needed to maintain liquid water in a particular lake environment under an early Martian atmosphere. Lake dynamics are particularly helpful in constraining past atmospheric conditions because lakes are highly sensitive to atmospheric forcing. Multiple climatic and lake-specific factors can influence the thermodynamics of a lake, including air temperature and lake size, depth, and salinity. To this end, we adapt, test, and describe a lake energy and water balance model previously used for Earth to simulate Martian climate and lake systems, LakeM^{2}ARS (Lake Modeling on Mars for Atmospheric Reconstructions and Simulations).

Lake models have been widely used to simulate and understand lake temperatures, water balance, and lake ice cover in different climate states on Earth (Braconnot et al., 2012; Dee et al., 2018; Hostetler & Bartlein, 1990; Huang et al., 2019; Morrill et al., 2001), but have heretofore never been used for investigating climate-lake interactions on other planets. To demonstrate the utility of our approach for constraining early Martian atmospheric conditions, we model a stable lake environment in Gale crater, Mars, and perform sensitivity tests with input parameters to narrow the estimated ranges of climate input variables required to maintain a liquid lake. Specifically, in-situ measurements and interpretations of Pahrump Hills are used here as parameters to run the lake model and serve as targets for output fields. We focus our analyses on three key questions: *1) What seasonal air temperatures are required to maintain a liquid lake? 2) How does salinity affect ice cover throughout the Martian year, and 3) How does lake geometry, including depth and surface area, impact lake conditions?* By exploring these key questions, we attempt to link paleoclimate evidence from Martian lakes to climate model boundary conditions to update our understanding of past hydrological cycling on Mars.

2. Methods

2.1. Lake Model Adaptation

The lake model modified for use in this study is the PRYSM v2.0 Lake Water and Energy Balance Model developed by Dee et al. (2018), originally published by Hostetler and Bartlein (1990) and Morrill et al. (2001). PRYSM is a proxy system model built to simulate relationships between climate inputs and paleoclimate proxy data in many forms - in this case, focusing on those housed in lacustrine environments (Dee et al., 2018). The PRYSM model, unlike other forward models for sedimentary proxy data, is modular and highly adaptable, designed to fit a wide variety of research questions in paleoclimatology. The flexible model framework allows for adaptation of the model to new environments, such as those hypothesized for early Mars.

This is the first study to drive an *intermediate*-complexity lake model with Mars GCM simulations (Evans et al., 2013; Trenberth, 1992). The appointment of "intermediate complexity" is taken from the climate modeling literature (Trenberth, 1992), and here refers to how accurately a given physical, biological, or chemical system is represented. A low-complexity model might simply apply a univariate linear regression, while a high-complexity model would thoroughly represent lake dynamical processes in four dimensions with high spatiotemporal resolution, accurate inputs, and large parameter sets, often employed for site-specific studies. The intermediate-complexity model introduced here strikes a balance between these end members to link the Martian climate and lake system processes to the best of our observational knowledge while allowing for uncertainties and sensitivity testing.

Fundamentally, the 1-D thermal and hydrologic model considers the conservation of energy and heat fluxes, temperature changes in the lake by eddy diffusion, salinity effects on water and evaporation, and lake ice cover. The outputs of seasonal lake conditions can then be evaluated to describe lake stability and characteristics that may be preserved in the geologic record. While we do not have paleoclimate proxy records from Mars comparable to those from Earth, we can use the energy and water balance capabilities of the PRYSM v2.0 framework for modeling lakes in a Martian environment (Figure 1). The governing equations of fluid dynamics are the same on both planets and with a few key parameter changes (e.g., gravity, the gas constant), we can effectively simulate massive crater lakes on Mars using geologic evidence and remote sensing data to estimate plausible ranges for atmospheric and surface conditions. We specify 10 years of spinup for the model to stabilize, and then we take the final two Mars years of the model output as our results.

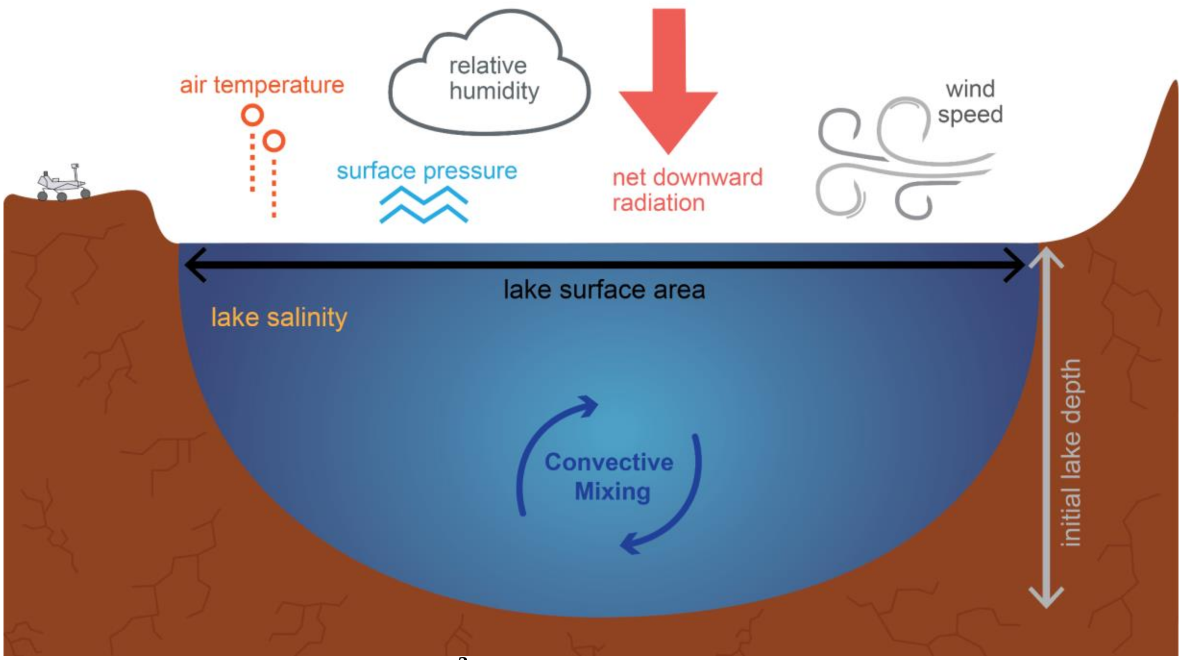

Figure 1. Schematic of the LakeM^{2}ARSmodel showing input model parameters. *Inputs and specified variables for the lake model include relative humidity (%), air temperature (°C), net downward radiation (W m^{-2}), pressure (mb), wind speed (m/s), lake salinity (ppt), initial lake depth (m), and lake surface area (m).*

The inputs and outputs for the LakeM^{2}ARS model used in this study are summarized in Table 1. The lake model requires six input variables from either meteorological observations or GCMs: near--surface air temperature, near-surface specific humidity, down-ward shortwave radiation (< 4.5 μm), downward longwave radiation (> 4.5 μm), near--surface wind speed, and surface pres-sure. The present version of the model primarily considers energy balance; future work will integrate water balance into the model in the form of input precipitation rate, basin runoff rate, and groundwater flux. Water balance and salinity can be on or off in the model, and for these purposes, our water balance flag will remain off in all model runs in this study, while the salinity flag will be toggled on and off. In the model runs to be discussed, where the salinity flag is toggled on, we specify salinity as an input parameter and the model will simulate the salt content in each vertical layer of the lake. Details on how to run the LakeM^{2}ARS model can be found in the supporting information (Text S1).

Table 1: Inputs and Outputs for the LakeM^{2}ARS model as developed by Hostetler and Barlein (1990), Morrill (2001), and Dee et al. (2018).

Model Inputs	**Model Outputs**
Year, latitude, longitude	Solar day (sol)
Air temperature at 2 meters (°C)	Lake surface temperature (°C)
Relative or Specific Humidity at 2 meters (%)	Lake evaporation (mm/day)
Wind Speed at 2 meters (m/s)	Average mixing depth (m)
Surface incident shortwave radiation (W/m^2)	Maximum mixed layer depth (m)
Downward longwave radiation (W/m^2)	Lake depth (m)
Surface Pressure (bar)	Ice fraction (0-1)
Lake depth and surface area (meters)	Ice height (m)
Initial lake salinity (ppt)	

Since this model was developed for Earth, some parameters had to be adapted to use the model for Mars and, more specifically, for Gale crater (Table 2). We make a common presumption that Mars' early atmosphere was CO_2-rich, as opposed to Earth's modern N_2- and O_2-rich atmosphere. This requires changing constants in the model that relate to atmospheric composition (Grott et al., 2011). The neutral drag coefficient, for one, relates to the resistance of the air above the lake to winds. This is influenced by the properties of the atmosphere, and due to the differences in atmospheric composition on Earth and Mars, we change the neutral drag coefficient to a value defined for Mars based on model experiments provided by Wordsworth et al. (2015). The specific heat capacity and gas constant for dry air were changed to the values for CO_2 to account for Mars' early atmosphere. The surface emissivity is the efficiency with which the longwave radiation makes it through the surface boundary layer above the lake and depends on the composition of the planet's surface; previous studies suggest Mars' emissivity ranges from 0.9 to 1 (Burgdorf, 2000; Christensen et al., 2004; Martínez et al., 2014). We select 0.95 as a reasonable estimate for surface longwave emissivity. The length of a year was adjusted in the model to be a Mars year by changing the degrees subtended per day. And, finally, the gravity of Mars is about one-third that of Earth's, or 3.71 m s^{-2}.

To model a lake in our specific study site of Gale crater, we select the latitude and longitude for the landing spot of the Curiosity rover, 4.59°S and 137.44°E (Seelos et al., 2014). We will also prescribe various Gale-specific initial lake depths, areas, and salinities, which will be discussed in section 2.3.

Table 2: Model Parameter values adapted to Mars and selected for Gale crater.

Model Parameter	**Unit**	**Modern Earth**	**Early Mars**
Obliquity	degree	23.4	35.0
Neutral drag coefficient	unitless	2.010^{-3}	2.7510^{-3}
Specific heat capacity for dry air	$J{\cdot}kg^{-1}{\cdot}K^{-1}$	1004.6	938.0
Specific gas constant for dry air	$Pa{\cdot}m^{3}{\cdot}kg^{-1}{\cdot}K^{-1}$	287.05	190.0
Longwave emissivity	unitless	0.97	0.95
Orbital degrees per day	degree	360/365	360/687
Gravity	$m{\cdot}s^{-2}$	9.81	3.71

Gale Crater Parameter	**Unit**	**Value**
Latitude	degree (N)	-4.59
Longitude	degree (E)	137.44
Lake depth	meters	*see section 2.3.1*
Lake surface area	meters	*see section 2.3.1*
Initial salinity	ppt	*see section 2.3.2*

Some model inputs, by contrast, are not easily adjusted for Mars (and, specifically, Gale crater). The model input fields outlined in Table 1 that are dependent on the climate of early Mars are likely to have been extremely variable and are therefore difficult to predict for early Mars (Kite, 2019). We used constant minimum, average, and maximum values for the input parameters for initial model testing based on previous work estimating these variables. Some parameters can be estimated on early Mars from geologic and geomorphic evidence including air temperature, and surface pressure (Kite, 2019). Other variables, for various reasons, are difficult to estimate for early Mars, including relative humidity, wind speed, and downwelling radiation; therefore, these values are estimated from ranges on present-day Mars and previous work with models (Kite et al., 2021; Martínez et al., 2021; Ramirez et al., 2020; Viúdez-Moreiras et al., 2019). Using these estimates, initial tests will consider endmembers of the input fields: air temperatures between -18°C to 40°C (Kite, 2019), surface pressures between 0.012 bar to 1 bar (Kite, 2019), relative humidity between 25% to 77% (Kite et al., 2021; Ramirez et al., 2020), wind speeds from 0 m/s to 30 m/s (Viúdez-Moreiras et al., 2019), downwelling shortwave radiation between 0 W/m^2 to 650 W/m^2 (Martínez et al., 2021), and downwelling longwave radiation from 20 W/m^2 to 120 W/m^2 (Martínez et al., 2021).

2.2. Climate Model Simulations & Seasonality

In order to simulate more realistic seasonally varying input fields for the lake model, we ran multiple simulations with the Mars Weather Research and Forecasting (MarsWRF) GCM, the Mars-specific adaptation of the planetWRF model (Richardson et al., 2007). The MarsWRF simulations used in this work are modified from the usual present-day values to simulate an early Mars environment (Table 3). First, while the current CO_2-dominant atmosphere of present-day Mars has an average surface pressure of around 0.007 bar (Martínez et al., 2017), the surface pressure used in the model is increased to 1 bar, to approximate a thicker atmosphere in the past (Warren et al., 2019). Next, in the GCM, Mars' obliquity is modified, as the obliquity is known to vary over geological timescales (Laskar et al., 2004; Ward, 1973). The obliquity is set to 35° which more closely reflects the long-term average value over Mars' history. Lastly, the sun's intensity is scaled to 75% of its current-day value to accommodate the faint young sun effect (Crowley, 1982), resulting in an average top-of-atmosphere solar flux of 442 W m^{-2}.

Table 3: Inputs for MarsWRF GCM Models

Symbol	Description	Unit	Tau = 3 Climate	Tau = 5.4 Climate
$p_{surface}$	Surface pressure	bar	1	1
ε	Planetary obliquity	degree	35	35
fys	Faint young sun factor	unitless	0.75	0.75
κ	Infrared absorption coefficient	$m^2\ kg^{-1}$	1.14×10^{-4}	2.01×10^{-5}
τ_{gray}	Gray gas opacity	unitless	3	5.4

To introduce additional warming in the model, a gray infrared absorptive gas is added, similar to previous methods simulating early Mars (Wordsworth et al., 2015). The gray gas acts as a proxy for the atmospheric composition that may have been warmed in the past, such as high concentrations of various greenhouse gasses (Ramirez et al., 2014) or high-altitude water-ice clouds (Kite et al., 2021). Two values for the infrared absorption coefficient were used in separate runs of the model, $1.12\text{x}10^{-4}$ and $2.0\text{x}10^{-4}\ m^2\ kg^{-1}$, corresponding to infrared gas opacities of $\tau_{gray} = 3$ and $\tau_{gray}= 5.4$ in a 1-bar atmosphere, respectively (Table 3).

The MarsWRF GCM is run with a horizontal resolution of 4° x 4°, yielding 90 points in longitude and 45 points in latitude. For this study, focused on Gale crater, we examined the model grid point (138°E/4°S) closest to the center of Gale crater (137.8°E/ 5.4°S). The vertical grid is split into 47 layers, up to an altitude of 120 km. A dynamical timestep of 180 seconds is used, and the model is run for nearly two Martian years. MarsWRF outputs used in this work begin at solar longitude (L_s) = 0° of the second modeled Martian Year. L_s is the Mars-Sun angle, measured from the Northern Hemisphere spring equinox where L_s = 0°.

Monthly average values of the daily fluxes are used to drive the lake model for the $\tau_{gray} = 3$ (cold) and $\tau_{gray} = 5.4$ (warm) climate simulations (Figure 2).

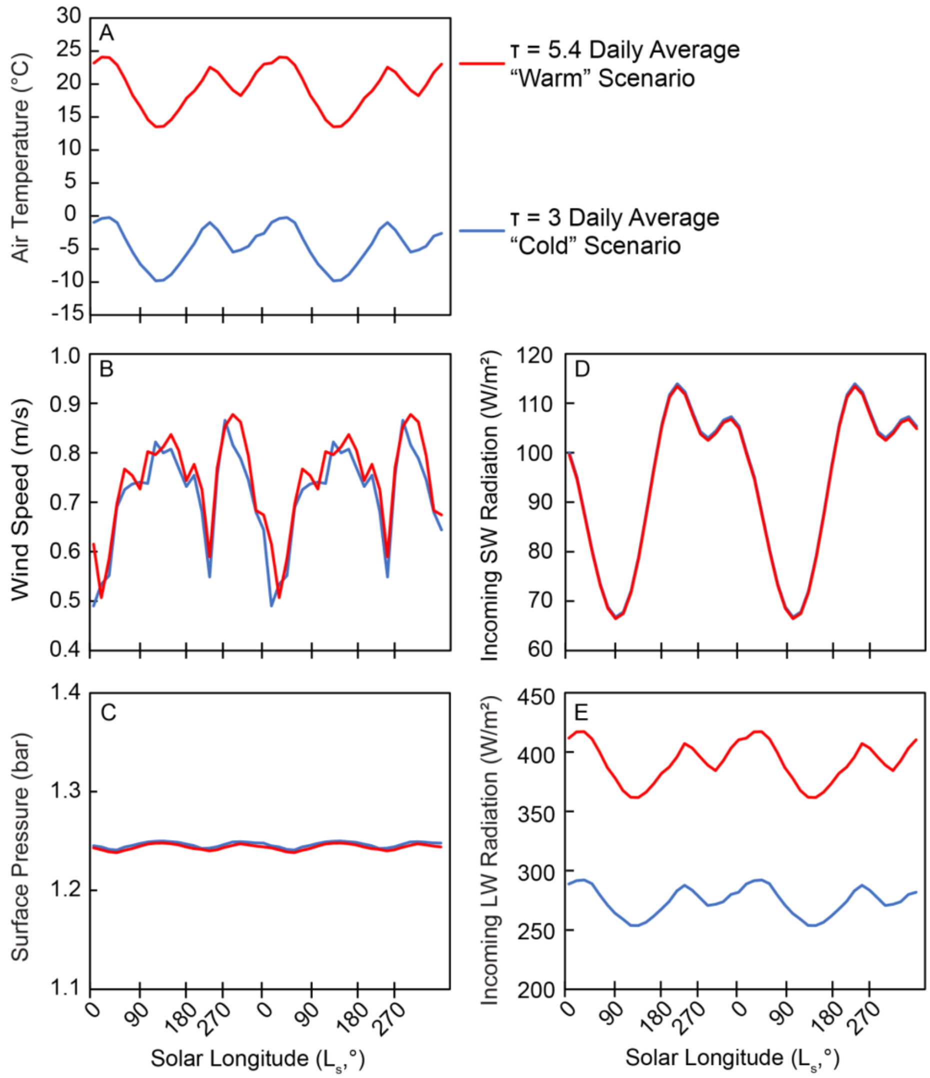

Figure 2. Climate variables simulated by the MarsWRF GCM over Gale crater area for input to the lake model. *Output daily averaged climate variables for τ_{gray} = 3 (blue, cold) and τ_{gray} = 5.4 (red, warm) MarsWRF models plotted against solar longitude (L_s,°), including: A) Air temperature (°C), B) Wind speed at 1.5 m above the surface (m/s), C) Surface pressure (bar), D) Shortwave radiation incident on the lake surface (W/m^2), and E) Longwave radiation incident on the lake surface (W/m^2).*

The only required climate input to the lake model not explicitly simulated in MarsWRF is relative humidity (RH); thus, we must establish a reasonable estimate for the amount of water vapor found in the early Martian atmosphere. Our approach is to explore conditions representative of a range of potential early climates by examining an 'arid' scenario with a fixed 5% RH and a 'humid' scenario with a fixed 70% RH. We assume the humidity value is constant over both time of day and season, acknowledging that such an assumption is likely unphysical; however, sensitivity tests have suggested only a minimal effect on our results from choosing a more complicated humidity time series scaled with temperature variations.

While early Mars climate scenarios are commonly referred to as 'cold and dry' or 'warm and wet' (with respect to global temperature relative to the melting point of water; see, e.g., Wordsworth [2016]), we have decoupled humidity from global mean temperatures. This allows us to represent four idealized climate states based on our choices of temperature and humidity. Our warm scenario is defined using the τ_{gray} = 5.4 average climate input while the cold scenario represents the τ_{gray} = 3 average values. Relative humidity is either constant at 5% for arid conditions or 70% for humid conditions. Thus, we can evaluate our lake response to four climate states: 1) cold and arid, 2) cold and humid, 3) warm and arid, and 4) warm and humid.

The simulated atmospheric seasonality from MarsWRF provides a best-informed guess at plausible early conditions on Mars (Figure 2). Using these inputs, we will attempt to identify the set of climatic conditions that support liquid water pooling at the surface, sustained throughout the year in lakes of variable size and salinity (as discussed in the following sections).

2.3. Lake-Specific Conditions: Lake Area and Salinity

2.3.1. Lake Size(s) in Gale Crater

Gale crater is among the best-studied sites on Mars as the landing site for the Mars Science Laboratory *Curiosity* rover, and it was the site of a large and long--lasting freshwater lake (Edgar et al., 2020; Grotzinger et al., 2015). *Curiosity's* investigations of the preserved stratigraphic record in the crater have shown evidence that ancient Gale contained small lakes with depths of about 5-10 m as preserved in the Bradbury and basal Murray formations (Grotzinger et al., 2015). An estimation of the surface area of a lake with 10 m depth on the floor of Gale today yields a surface area of 1855 km^2 (this is certainly oversimplified and not directly representative of the topography billions of years ago, but a first approximation of lake scale), so we use these parameters to describe a small lake endmember in Gale. Geomorphic studies of the modern topography of Gale indicate that there may have been a later high lake stand of a more recent lake with mean depths up to 700 m and surface area reaching 5832 km^2 (Palucis et al., 2016). Thus, we opted to test these two described lake sizes as 'endmember' scenarios: the small lake system has an initial depth of 10 m (Grotzinger et al., 2015) and a surface area of 1855 km^2, while the large lake system is initialized at 700 m depth and has a prescribed surface area of 5832 km^2 as reported by Palucis et al. (2016).

2.3.2. Variable Salinity of Gale Crater Lake(s)

Salinity directly controls the freezing point of water and could have major impacts on lake stability and lake surface temperature. To test how salinity influences the stability of simulated lake systems, the lake model's salinity flag was toggled on, allowing salt content to fluctuate within the water column and via surface evaporation. Freezing point depression, or the decrease in the freezing point of water due to the addition of salts, is characterized at low salt concentrations by thermodynamic equations and properties of pure water (Lamas et al., 2022). The equation for freezing point depression has previously been adapted to fit models of subglacial lakes and high salt concentration scenarios (Lamas et al., 2022; Thoma et al., 2010), but in-situ evidence from Gale crater indicates the lake likely maintained relatively freshwater conditions (Stack et al., 2019). The exact salinity of past Gale lakes, however, could have ranged from freshwater (~1000 kg m^{-3} or ~4 ppt) to that of the Earth's oceans (1027 kg m^{-3} or ~40 ppt), with more saline conditions less probable (Stack et al., 2019). Given the range of possible salinity and its importance to lake conditions, we test four salinity scenarios: freshwater (salinity = 0.5 ppt), brackish water (15 ppt), saline water (35 ppt), and very saline water (50 ppt). While freshwater and brackish conditions are more supported by geologic evidence (Stack et al., 2019), we also aim to explore a larger parameter space enabling robust evaluation of plausible conditions in Gale paleolakes.

3. Results

3.1. Model Validation

Initial testing of the LakeM^{2}ARS model focused on ensuring the lake model would run without error under constant Martian planetary parameters and paleoclimatic conditions. Using constant input fields within the reported range of input variables, we tuned and debugged the model to simulate lake conditions assuming no seasonality. Firstly, the model was tested with two air temperatures (-18 and 40 °C), two surface pressure values (0.012 and 1 bar), and two wind speed values (0 and 30 m/s) with all other inputs held to an average value determined by reported ranges of these variables for early Mars. These simulations with constant input fields were important for validating model performance, and ensuring physically meaningful results. As expected, increasing air temperature increased lake surface temperature, mixing depth, and lake evaporation. Lower air pressure led to higher lake evaporation. Lastly, increasing wind speed lowered the lake surface temperature and significantly increased mixing depth and lake evaporation. While these tests are simplistic, they confirmed the lake model produces expected results under Martian climate conditions as input parameters are varied.

Next, with the salinity flag toggled on, we tested the modeled lake using four arbitrary salinity values (0, 4, 80, or 156 ppt) while simultaneously varying air temperature (-18, 0, or 11 °C). With a constant air temperature, increased salinity values resulted in decreased lake surface temperature, decreased ice height, and decreased evaporation. These are expected outcomes of increased lake salinity and confirm our model salinity flag is functioning as expected (Wen et al., 2022).

Preliminary sensitivity tests with constant inputs established reasonable model functionality; we next proceeded with a suite of sensitivity tests using more realistic Martian climate states.

3.2. Sensitivity to Seasonality, Salinity, and Lake Size

Tests for variable climate conditions and initial salinity required implementing the MarsWRF GCM outputs as our climate inputs and turning on variable salinity in the lake model. As outlined in section 2.2, we ran tests for combinations of our four climate states (cold and arid, cold and humid, warm and arid, and warm and humid), four initial salinity conditions (0, 15, 35, and 50 ppt), and two sizes of lake system to generate a total of n = 32 lake model simulations. LakeM^{2}ARS will output a time series with values calculated for each monthly time step for all variables outlined in Table 1 (Moreland et al., 2024). We focus on two output fields given their relevance for maintaining a liquid lake system: lake surface temperature and evaporation, for which long-term (two Mars years) averages are shown in Figure 3 to summarize the key results of the sensitivity tests. Additional LakeM^{2}ARS outputs are presented in the Supporting Information.

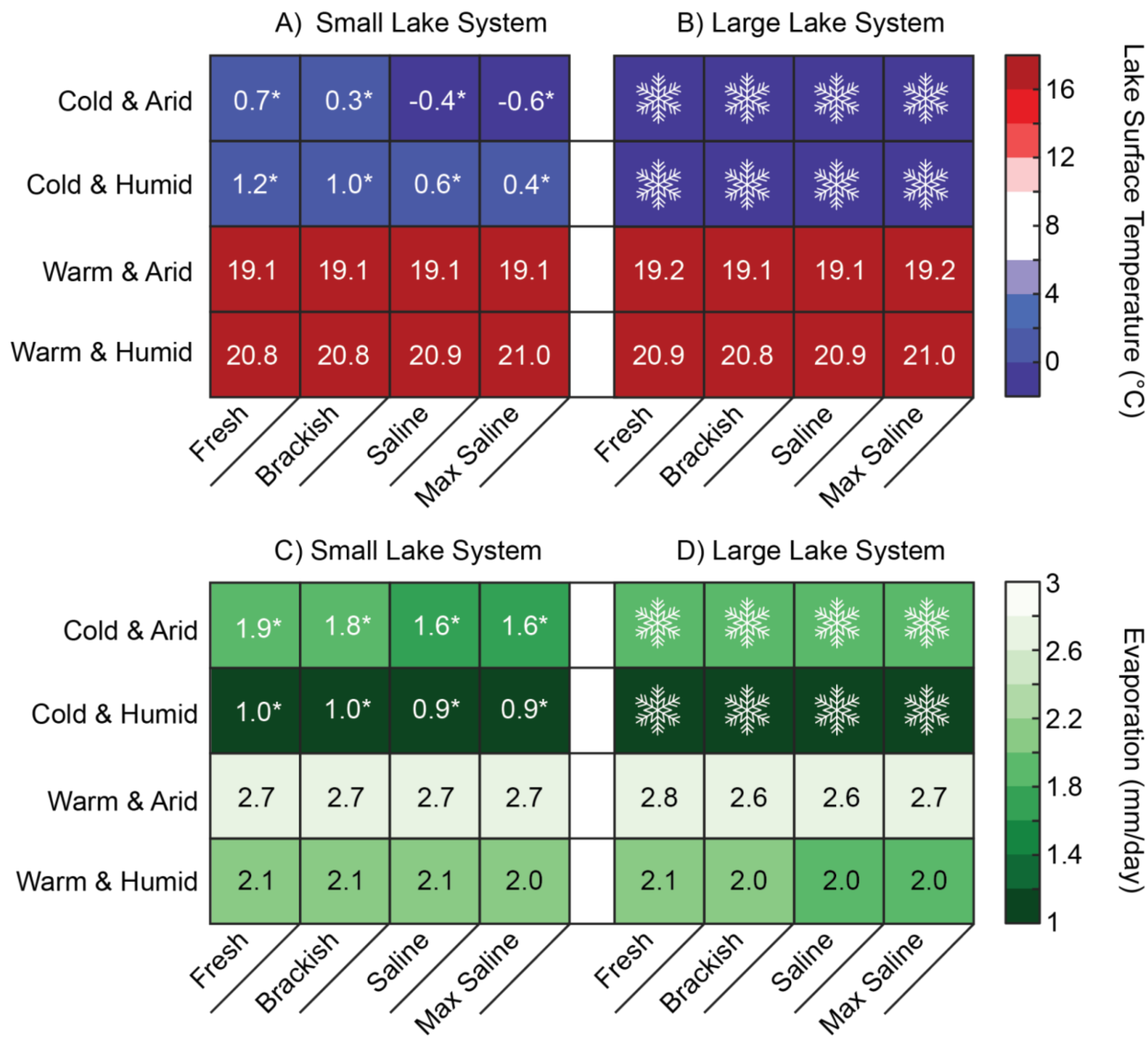

Figure 3. Annual average results of variable climate input, salinity, and lake system size on average output lake surface temperature (°C) and evaporation (mm/day). *A) 2-year averaged lake surface temperature in a small lake system for variable climate conditions, B) Average lake surface temperature in a large lake system, C) Average evaporation in a small lake system for variable climate conditions, and D) Average evaporation in a large lake system. Conditions with a snowflake indicate the lake was entirely ice-covered for the entire duration of the model run. * Indicates conditions with seasonally variable ice cover.*

Under non-frozen conditions, lake surface temperatures follow air temperature forcing (Figures 3A & 3B). Humid conditions cause the lake surface temperature to be slightly warmer than the arid conditions, and starting salinity appears to have minor or non-linear effects on the lake surface temperature. Evaporation increases with increasing air temperature and decreases with increasing humidity (Figures 3C & 3D). The size of the lake system exerts clear controls on simulated lake temperatures and freezing conditions in the lakes: the small system simulations show seasonally variable ice cover in the cold simulations; however, with the same forcing, the large system stays frozen no matter the salinity (Figure 3). Overall, our sensitivity tests show the resulting lake is indeed influenced by the initial climate forcings and the size of the lake, while the effects of salinity require further tests to fully understand.

As discussed in Section 1, we are interested in investigating conditions that align with both the geologic record and estimates for early Martian climate. Specifically, the geologic constraints indicate that the lake is smaller, ice-free for some portion of the year, has near-freshwater salinity, and exists continuously for 10^3 years or more (for the present model, we represent this as a steady existence over two Mars years). Paleoclimate and geochemical constraints on Mars emphasize the need to minimize the need for an exaggerated greenhouse effect, i.e., our 'cold' climate conditions with lower atmospheric opacity. These criteria are met with the small lake system, freshwater or brackish salinity, with the cold climate inputs. Our sensitivity tests show the combination of these conditions produces a lake with a seasonally liquid lake, and any warmer temperatures would theoretically decrease the amount of seasonal ice cover and increase the time of liquid state (Figure 3).

3.3. Time Series Investigation of a Small Lake System

To assess how atmospheric forcing affected the simulated lake conditions throughout the Martian year, we evaluate the time series (two Mars years) of lake surface temperature (°C), evaporation rate (mm/day), and ice height (m) for the small lake system for all climate conditions (Figure 4). As discussed in section 3.2, we are most interested in the freshwater and brackish salinity conditions in order to best match the geologic record, thus we focus on those two salinity conditions for the time series investigation (Figure 4). Other outputs not shown here include average and maximum mixing depth, latent and sensible heat flux out of the lake, and shortwave and longwave radiation out of the lake; figures of additional output fields for all model runs are in Figures S1-S4.

Note that temperatures flatlining near 0°C indicate a sustained frozen lake surface; lake surface temperatures remain constant when there is built-up ice on the lake (Figures 4A & 4C). This behavior in lake surface temperature is evident in the cold conditions, under both fresh and brackish conditions – the scenarios that also had the largest amount of ice for the most extended period of time. However, we also observe periods of ice melting (decrease in ice height) that correlate with small increases in lake surface temperature (Figures 4A & 4C). There is a minor influence of salinity visible with the frozen conditions; the cold and brackish conditions reach slightly lower temperatures than the cold and freshwater (Figure 4A) and the freshwater conditions are able to reach slightly higher ice height than their brackish counterparts (Figure 4C). Additionally, humidity plays a role in the ice cover, with higher humidity causing less ice cover on the lake (Figure 4C).

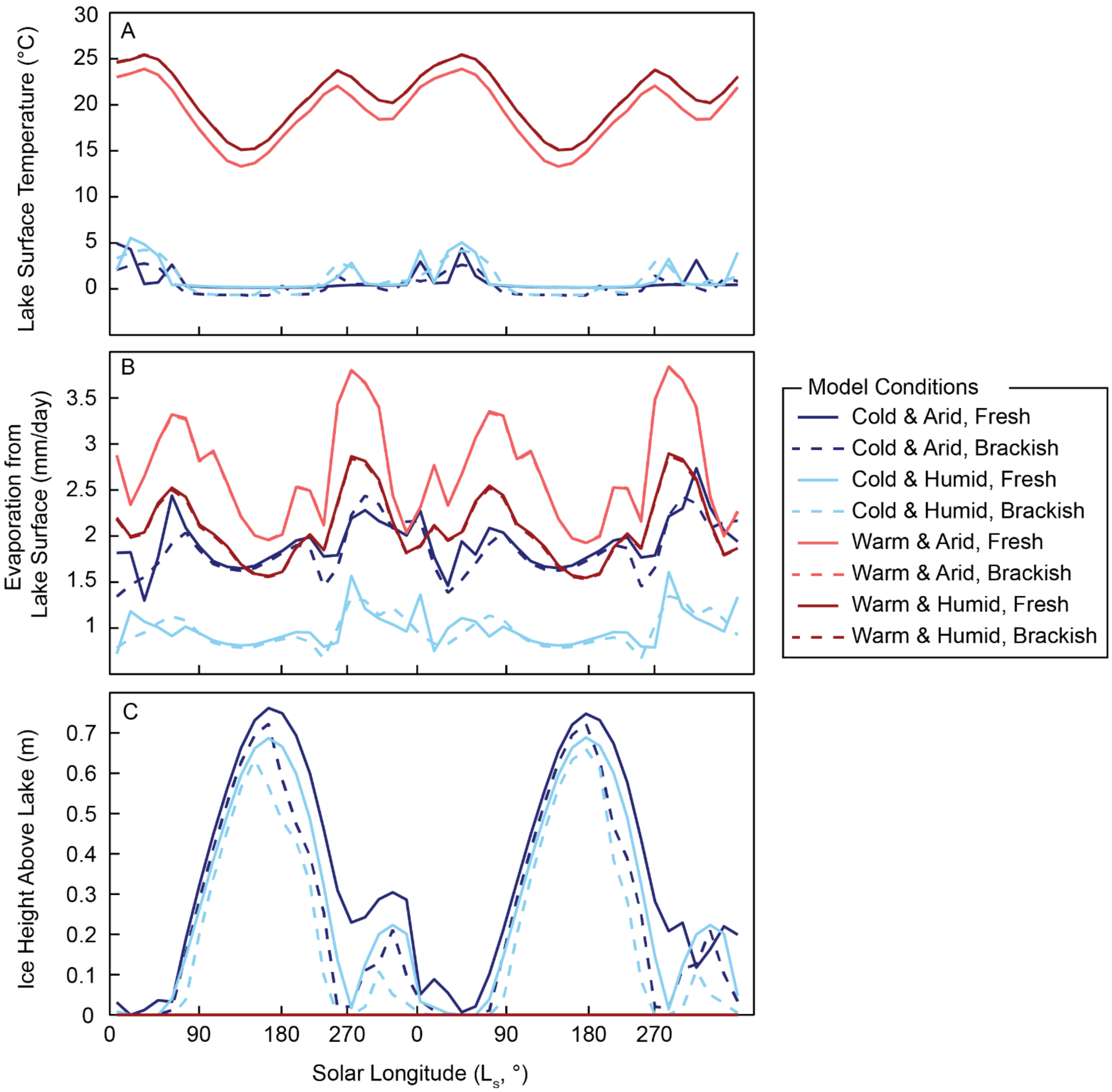

Figure 4. Time series of select output variables from LakeM^{2}ARS for a small lake system with variable climate inputs and salinity values. *A) Lake surface temperature (°C) for all conditions, C) Evaporation from lake surface (mm/day), and C) Ice height above the lake (m).*

The warm, non-frozen conditions, on the other hand, reach significantly higher lake surface temperature than the cold conditions, which are expected from the climate having the warmest air temperature inputs (Figure 4A). These conditions are completely free of ice and the lake surface temperatures closely track air temperatures, occasionally exceeding input air temperatures (Figure 4A).

The evaporation rates generally peak when lake surface temperatures peak, an expected relationship as a warmer lake surface supports increased evaporation rates (Figure 4B). In some cases, primarily in warm conditions, there is a slight delay in peak evaporation rate compared to the peak in lake surface temperature (Figures 4A & 4B). As seen in Figures 3C & 3D, the humid conditions cause lower evaporation rates than the arid counterparts, and salinity does not have a significant effect on evaporation rates (Figure 4B).

3.4. Time Series Investigation of a Large Lake System

Simulations for the large lake system suggest favorable conditions for liquid lakes exist for all salinities in warm conditions (Figure 3). Thus, we investigate the time series for the warm conditions in the large lake, showing lake surface temperature (°C) and evaporation rate (mm/day) in Figure 5. Ice height is not included here because there was no ice buildup in these conditions; figures of additional output fields for all model runs are in Figures S5-S8.

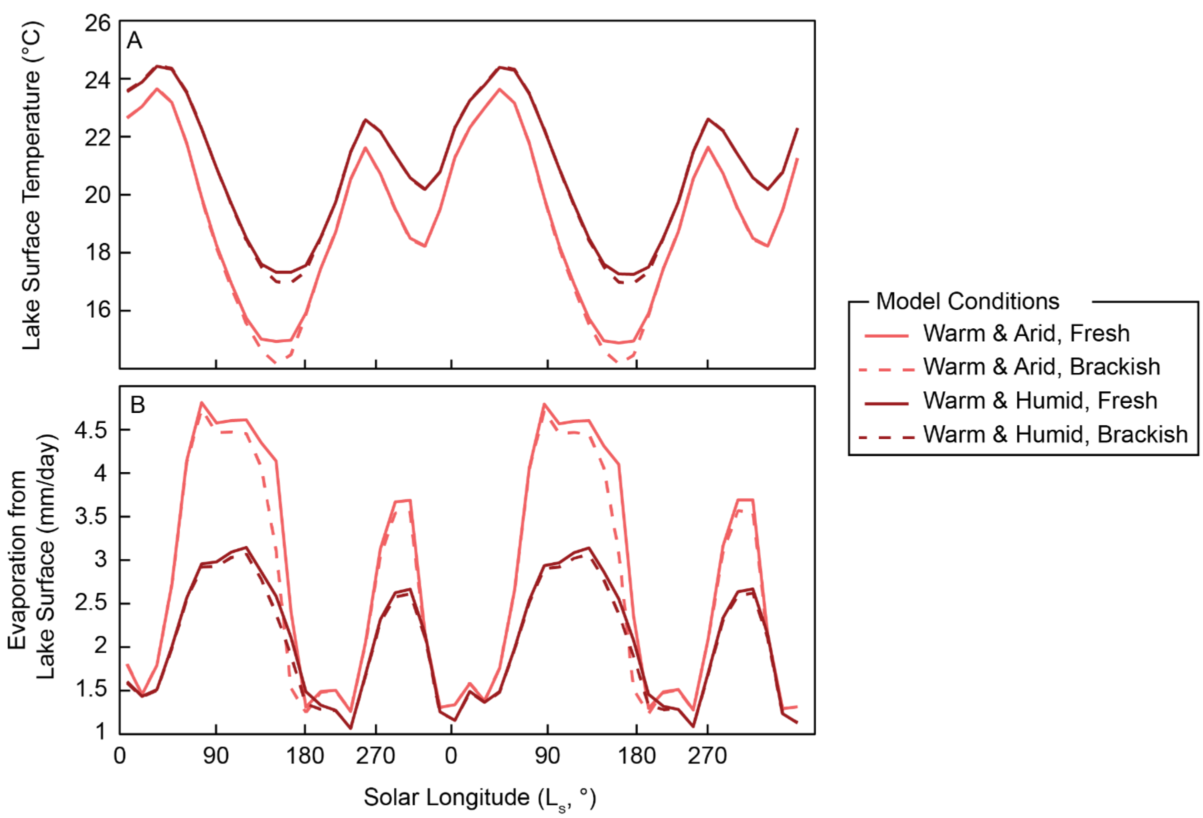

Figure 5. Time series of select output variables from LakeM^{2}ARS for a large lake system with variable climate inputs and salinity values. *A) Lake surface temperature (°C) for all conditions and B) Evaporation from lake surface (mm/day).*

All conditions have lake surface temperatures that closely match air temperature forcings, while the humid conditions reach higher lake surface temperatures compared to the arid conditions (Figure 5A). These lake surface temperatures track or slightly exceed air temperatures, and in this large lake, the peak in lake surface temperature lags the seasonal peak in input air temperature by approximately 30 sols. This temperature lag was not observed in the small lake and highlights that the larger lake takes longer to reach thermal equilibrium with surface air temperatures compared to the smaller lake. Again, salinity does not have an obvious effect on the lake surface temperature in the large lake besides allowing lake surface temperatures to reach slightly lower in the brackish conditions compared to the fresh conditions (Figure 5A).

There is a significant effect of humidity on evaporation rates in the large lake; higher humidity decreases the peak evaporation rate by close to 2 mm/day (Figure 5B). Higher salinity (brackish) conditions mildly lower the evaporation rates as well. Evaporation rates reach maxima just before lake surface temperature peaks, possibly due to evaporation rates in the large lake responding more to air temperatures than lake surface temperatures but more tests would be required to understand the relationship fully.

Discussion & Future Work

The Mars of today and the past are two very different worlds, and significant uncertainty exists in explaining how an active hydrological cycle could have been maintained on Mars given its small size and distance from the sun. Martian climate models, to date, have not been able to simulate or explain a set of realistic atmospheric conditions required to generate stable liquid water lakes on the surface of early Mars. Our adapted, intermediate complexity water and energy balance lake model for Mars provides critical constraints on the early Martian hydrological cycle and explicitly merges localized climate model experiments with geologic evidence. Our initial tests of Gale crater lakes confirm LakeM^{2}ARS successfully simulates lakes and lacustrine environments on Mars; furthermore, the adaptation to Martian climate conditions has yielded a model that can simulate dynamic lakes with plausible planetary and paleoclimate conditions estimated for ancient Mars. Our sensitivity experiments varying climate inputs, salinity, and lake size allowed us to estimate conditions yielding ice vs. ice-free conditions for lakes in Gale crater, the site of the *Curiosity* rover. We explored our three key questions:

1) What seasonal air temperatures are required to maintain a liquid lake?

To support a liquid lake with seasonal ice cover, the air temperatures can seasonally reach just about freezing (0°C), but the lake has to be small; a larger lake will remain fully frozen year-round. To achieve no ice cover at all throughout the year regardless of lake size and salinity, the lake requires a warm climate with air temperatures above freezing.

2) How does salinity affect ice cover throughout the Martian year?

The cold conditions in the small lake produced seasonal variability in ice cover, and increasing the salinity decreases the amount of ice that forms on the lake. The large system either experienced completely frozen conditions in cold air temperatures or completely ice-free conditions in warmer air temperatures.

Finally, *3) how does lake geometry, including depth and surface area, impact lake conditions?*

Ice-free conditions in the small lake system were easier to achieve and occurred more frequently than in the large system. The small lake size thermally equilibrates more rapidly with warming air temperatures and can thaw more quickly compared to the large system.

The successful adaptation of an Earth-based lake model into a lake model for early Mars provides opportunities for a large array of future studies. For the initial model building in this study, we did not interrogate water balance nor experiment with altered precipitation, runoff, or groundwater inflows. Subsequent tests will apply varying seasonal precipitation, runoff, and groundwater inflows to simulate changes in lake level and the entire hydrologic balance of the lake system. Additional model variables, such as the albedo of snow, can be altered to understand how these parameterizations affect the longevity of a liquid water lake. With specific relevance to Gale crater, we plan to implement a module for groundwater fluxes as multiple studies have indicated that warm groundwater was potentially an important factor in Gale crater (Gasda et al., 2022; Rampe et al., 2020; Thorpe et al., 2022).

LakeM^{2}ARS facilitates direct comparison to available in situ geochemical and stratigraphic data from the *Curiosity* rover in Gale crater. These studies can expand to the numerous, well-studied sites of paleolakes on Mars such as Jezero crater, the site of the *Perseverance* rover, and Eberswalde crater (Goudge et al., 2015; Grotzinger et al., 2015; Irwin et al., 2015). These locations provide clear targets for climate models to investigate the atmospheric conditions that support a lake’s thermodynamic conditions, namely, liquid water at the lake's surface, and comparisons amongst sites could give a better planet-wide view of early Mars' hydrologic cycle.

4. Conclusion

Our publicly available, open-source model, LakeM^{2}ARS, can be adapted to any paleolake site on Mars with a few key parameter changes (Table 2) and atmospheric simulations via GCM runs. We hope the documentation provided with our work will encourage broad use in the Martian hydrology community. LakeM^{2}ARS provides a new and promising avenue for refining estimates of hydrological cycle activity, climate mechanisms, duration of lake stability, and atmospheric temperatures and pressures on early Mars. By identifying the range of climate variables required to enable the lake deposits in Gale, this work takes a first step towards refining constraints on Martian paleoclimate grounded in the geologic record. We hope to continue providing improved estimates of Mars' paleoclimate conditions, specifically surrounding water balance in large crater lakes. This information is needed to inform physics and boundary condition choices in Mars paleoclimate modeling work and bolster our understanding of early Mars's conditions, hydrology, and potential habitability.

Data Availability Statement

Input data files used to run the LakeM^{2}ARS model and output data used to generate figures are provided in Moreland et al. (2024) [Data Set]. The model code is available through GitHub (https://github.com/sylvia-dee/PRYSM).

Acknowledgments

This work was supported by the Rice Faculty Initiative Fund awarded to S.D. and K.S., which supported S.D., K.S., E.M., and Y.J. A portion of this work was carried out at the Jet Propulsion Laboratory, California Institute of Technology, under a contract with the National Aeronautics and Space Administration (80NM0018D0004). Resources supporting this work were provided by the NASA High-End Computing (HEC) program through the NASA Advanced Supercomputing (NAS) Division at Ames Research Center. J.M. and G.B. were supported by a Canadian Space Agency MSL Participating Scientist Grant. The authors thank Carrie Morrill for her helpful guidance in running and adapting the lake model.

References

Braconnot, P., Harrison, S. P., Kageyama, M., Bartlein, P. J., Masson-Delmotte, V., Abe-Ouchi, A., et al. (2012). Evaluation of climate models using palaeoclimatic data. *Nat. Clim. Chang.*, *2*(6), 417–424.

Burgdorf, M. (2000). ISO observations of mars: An estimate of the water vapor vertical distribution and the surface emissivity. *Icarus*, *145*(1), 79–90.

Carr, M. H. (1987). Water on mars. *Nature*, *326*(6108), 30–35.

Christensen, P. R., Wyatt, M. B., Glotch, T. D., Rogers, A. D., Anwar, S., Arvidson, R. E., et al. (2004). Mineralogy at Meridiani Planum from the Mini-TES Experiment on the Opportunity Rover. *Science*, *306*(5702), 1733–1739.

Crowley, T. J. (1982). *The Geologic Record of Climatic Change*.

Davis, J. M., Gupta, S., Balme, M., Grindrod, P. M., Fawdon, P., Dickeson, Z. I., & Williams, R. M. E. (2019). A diverse array of fluvial depositional systems in Arabia Terra: Evidence for mid-Noachian to early Hesperian rivers on Mars. *J. Geophys. Res. Planets*, *124*(7), 1913–1934.

Dee, S. G., Russell, J. M., Morrill, C., Chen, Z., & Neary, A. (2018). PRYSM v2.0: A proxy system model for lacustrine archives. *Paleoceanogr. Paleoclimatology*, *33*(11), 1250–1269.

Edgar, L. A., Fedo, C. M., Gupta, S., Banham, S. G., Fraeman, A. A., Grotzinger, J. P., et al. (2020). A lacustrine paleoenvironment recorded at Vera RubinRidge, gale crater: Overview of the sedimentology and stratigraphy observed by the mars ScienceLaboratory curiosity rover. *J. Geophys. Res. Planets*, *125*(3).

Evans, M. N., Tolwinski-Ward, S. E., Thompson, D. M., & Anchukaitis, K. J. (2013). Applications of proxy system modeling in high resolution paleoclimatology. *Quat. Sci. Rev.*, *76*, 16–28.

Fassett, C. I., & Head, J. W. (2008). The timing of martian valley network activity: Constraints from buffered crater counting. *Icarus*, *195*(1), 61–89.

Forget, F., Wordsworth, R., Millour, E., Madeleine, J.-B., Kerber, L., Leconte, J., et al. (2013). 3D modelling of the early martian climate under a denser CO2 atmosphere: Temperatures and CO2 ice clouds. *Icarus*, *222*(1), 81–99.

Gasda, P. J., Comellas, J., Essunfeld, A., Das, D., Bryk, A. B., Dehouck, E., et al. (2022). Overview of the morphology and chemistry of diagenetic features in the clay-rich glen torridon unit of gale crater, mars. *J. Geophys. Res. Planets*, *127*(12).

Golombek, M., Grant, J., Kipp, D., Vasavada, A., Kirk, R., Fergason, R., et al. (2012). Selection of the mars science laboratory landing site. *Space Sci. Rev.*, *170*(1–4), 641–737.

Goudge, T. A., Mustard, J. F., Head, J. W., Fassett, C. I., & Wiseman, S. M. (2015). Assessing the mineralogy of the watershed and fan deposits of the Jezero crater paleolake system, Mars. *Journal of Geophysical Research: Planets*, *120*(4), 775–808. https://doi.org/10.1002/2014JE004782

Goudge, T. A., Morgan, A. M., Stucky de Quay, G., & Fassett, C. I. (2021). The importance of lake breach floods for valley incision on early Mars. *Nature*, *597*(7878), 645–649.

Grant, J. A., Golombek, M. P., Wilson, S. A., Farley, K. A., Williford, K. H., & Chen, A. (2018). The science process for selecting the landing site for the 2020 Mars rover. *Planet. Space Sci.*, *164*, 106–126.

Grott, M., Morschhauser, A., Breuer, D., & Hauber, E. (2011). Volcanic outgassing of CO2 and H2O on Mars. *Earth Planet. Sci. Lett.*, *308*(3), 391–400.

Grotzinger, J. P., Crisp, J., Vasavada, A. R., Anderson, R. C., Baker, C. J., Barry, R., et al. (2012). Mars science laboratory mission and science investigation. *Space Sci. Rev.*, *170*(1–4), 5–56.

Grotzinger, J. P., Gupta, S., Malin, M. C., Rubin, D. M., Schieber, J., Siebach, K., et al. (2015). Deposition, exhumation, and paleoclimate of an ancient lake deposit, Gale crater, Mars. *Science*, *350*(6257), aac7575.

Harri, A.-M., Genzer, M., Kemppinen, O., Kahanpää, H., Gomez-Elvira, J., Rodriguez-Manfredi, J. A., et al. (2014). Pressure observations by the Curiosity rover: Initial results. *J. Geophys. Res. Planets*, *119*(1), 82–92.

Hostetler, S. W., & Bartlein, P. J. (1990). Simulation of lake evaporation with application to modeling lake level variations of Harney-Malheur Lake, Oregon. *Water Resour. Res.*, *26*(10), 2603–2612.

Huang, W., Cheng, B., Zhang, J., Zhang, Z., Vihma, T., Li, Z., & Niu, F. (2019). Modeling experiments on seasonal lake ice mass and energy balance in the Qinghai–Tibet Plateau: a case study. *Hydrol. Earth Syst. Sci.*, *23*(4), 2173–2186.

Irwin, R. P., Lewis, K. W., Howard, A. D., & Grant, J. A. (2015). Paleohydrology of Eberswalde crater, Mars. *Geomorphology*, *240*, 83–101.

Jakosky, B. M., Brain, D., Chaffin, M., Curry, S., Deighan, J., Grebowsky, J., et al. (2018). Loss of the Martian atmosphere to space: Present-day loss rates determined from MAVEN observations and integrated loss through time. *Icarus*, *315*, 146–157.

Kasting, J. F. (1991). CO2 condensation and the climate of early Mars. *Icarus*, *94*, 1–13.

Kite, E. S. (2019). Geologic Constraints on Early Mars Climate. *Space Sci. Rev.*, *215*(1), 10.

Kite, E. S., Steele, L. J., Mischna, M. A., & Richardson, M. I. (2021). Warm early Mars surface enabled by high-altitude water ice clouds. *Proc. Natl. Acad. Sci. U. S. A.*, *118*(18).

Kling, A. M., Haberle, R. M., McKay, C. P., Bristow, T. F., & Rivera-Hernández, F. (2020). Subsistence of ice-covered lakes during the Hesperian at Gale crater, Mars. *Icarus*, *338*, 113495.

Lamas, C. P., Vega, C., & Noya, E. G. (2022). Freezing point depression of salt aqueous solutions using the Madrid-2019 model. *J. Chem. Phys.*, *156*(13), 134503.

Laskar, J., Correia, A. C. M., Gastineau, M., Joutel, F., Levrard, B., & Robutel, P. (2004). Long term evolution and chaotic diffusion of the insolation quantities of Mars. *Icarus*, *170*(2), 343–364.

Mangold, N., Gupta, S., Gasnault, O., Dromart, G., Tarnas, J. D., Sholes, S. F., et al. (2021). Perseverance rover reveals an ancient delta-lake system and flood deposits at Jezero crater, Mars. *Science*, *374*(6568), 711–717. https://doi.org/10.1126/science.abl4051

Martínez, G. M., Rennó, N., Fischer, E., Borlina, C. S., Hallet, B., de la Torre Juárez, M., et al. (2014). Surface energy budget and thermal inertia at Gale Crater: Calculations from ground-based measurements. *J Geophys Res Planets*, *119*(8), 1822–1838.

Martínez, G. M., Newman, C. N., De Vicente-Retortillo, A., Fischer, E., Renno, N. O., Richardson, M. I., et al. (2017). The modern near-surface martian climate: A review of in-situ meteorological data from viking to curiosity. *Space Sci. Rev.*, *212*(1–2), 295–338.

Martínez, G. M., Vicente-Retortillo, A., Vasavada, A. R., Newman, C. E., Fischer, E., Rennó, N. O., et al. (2021). The surface energy budget at gale crater during the first 2500 sols of the mars science laboratory mission. *J. Geophys. Res. Planets*, *126*(9).

Moreland, E., Dee, S., Jiang, Y., Bischof, G., Mischna, M., & Hartigan, N. (2024). Lake Modeling on Mars for Atmospheric Reconstructions and Simulations (LakeM2ARS): An intermediate-complexity model for simulating Martian lacustrine environments [Data set]. Zenodo. https://doi.org/10.5281/zenodo.10581393

Morrill, C., Small, E. E., & Sloan, L. C. (2001). Modeling orbital forcing of lake level change: Lake Gosiute žEocene/ , North America.

Palucis, M. C., Dietrich, W. E., Williams, R. M. E., Hayes, A. G., Parker, T., Sumner, D. Y., et al. (2016). Sequence and relative timing of large lakes in Gale crater (Mars) after the formation of Mount Sharp. *J. Geophys. Res. Planets*, *121*(3), 472–496.

Ramirez, R. M., & Craddock, R. A. (2018). The geological and climatological case for a warmer and wetter early Mars. *Nat. Geosci.*, *11*(4), 230–237.

Ramirez, R. M., Kopparapu, R., Zugger, M. E., Robinson, T. D., Freedman, R., & Kasting, J. F. (2014). Warming early Mars with CO2 and H2. *Nat. Geosci.*, *7*(1), 59–63.

Ramirez, R. M., Craddock, R. A., & Usui, T. (2020). Climate Simulations of Early Mars With Estimated Precipitation, Runoff, and Erosion Rates. *Journal of Geophysical Research: Planets*, *125*(3), e2019JE006160.

Rampe, E. B., Blake, D. F., Bristow, T. F., Ming, D. W., Vaniman, D. T., Morris, R. V., et al. (2020). Mineralogy and geochemistry of sedimentary rocks and eolian sediments in Gale crater, Mars: A review after six Earth years of exploration with Curiosity. *Geochemistry*, *80*(2), 125605. https://doi.org/10.1016/j.chemer.2020.125605

Richardson, M. I., Toigo, A. D., & Newman, C. E. (2007). PlanetWRF: A general purpose, local to global numerical model for planetary atmospheric and climate dynamics. *Journal of Geophysical Reserach*, *112*(E09001).
Scheller, E. L., Ehlmann, B. L., Hu, R., Adams, D. J., & Yung, Y. L. (2021). Long-term drying of Mars by sequestration of ocean-scale volumes of water in the crust. *Science*, *372*(6537), 56–62.
Seelos, K. D., Seelos, F. P., Viviano-Beck, C. E., & others. (2014). Mineralogy of the MSL Curiosity landing site in Gale crater as observed by MRO/CRISM. *Geophysical Research Letters*, *41*(14), 4880–4887.
Stack, K. M., Grotzinger, J. P., Lamb, M. P., Gupta, S., Rubin, D. M., Kah, L. C., et al. (2019). Evidence for plunging river plume deposits in the Pahrump Hills member of the Murray formation, Gale crater, Mars. *Sedimentology*, *66*(5), 1768–1802.
Stucky de Quay, G., Kite, E. S., & Mayer, D. P. (2019). Prolonged fluvial activity from channel-fan systems on mars. *J. Geophys. Res. Planets*, *124*(11), 3119–3139.
Thoma, M., Grosfeld, K., Smith, A. M., & Mayer, C. (2010). A comment on the Equation of State and the freezing point equation with respect to subglacial lake modelling. *Earth Planet. Sci. Lett.*, *294*(1), 80–84.
Thorpe, M. T., Bristow, T. F., Rampe, E. B., Tosca, N. J., Grotzinger, J. P., Bennett, K. A., et al. (2022). Mars science laboratory CheMin data from the Glen torridon region and the significance of lake-groundwater interactions in interpreting mineralogy and sedimentary history. *J. Geophys. Res. Planets*, *127*(11).
Trenberth, K. E. (1992). *Climate system modeling*. Cambridge University Press.
Viúdez-Moreiras, D., Gómez-Elvira, J., Newman, C. E., Navarro, S., Marin, M., Torres, J., & de la Torre-Juárez, M. (2019). Gale surface wind characterization based on the Mars Science Laboratory REMS dataset. Part II: Wind probability distributions. *Icarus*, *319*, 645–656.
Ward, W. R. (1973). Large-scale variations in the obliquity of Mars. *Science*, *181*(4096), 260–262.
Warren, A. O., Kite, E. S., Williams, J.-P., & Horgan, B. (2019). Through the thick and thin: New constraints on mars paleopressure history 3.8 – 4 Ga from small exhumed craters. *J. Geophys. Res. Planets*, *124*(11), 2793–2818.
Wordsworth, R. D. (2016). The Climate of Early Mars.
Wordsworth, R. D., Kerber, L., Pierrehumbert, R. T., Forget, F., & Head, J. W. (2015). Comparison of “warm and wet” and “cold and icy” scenarios for early Mars in a 3-D climate model. *J. Geophys. Res. Planets*, *120*(6), 1201–1219.